

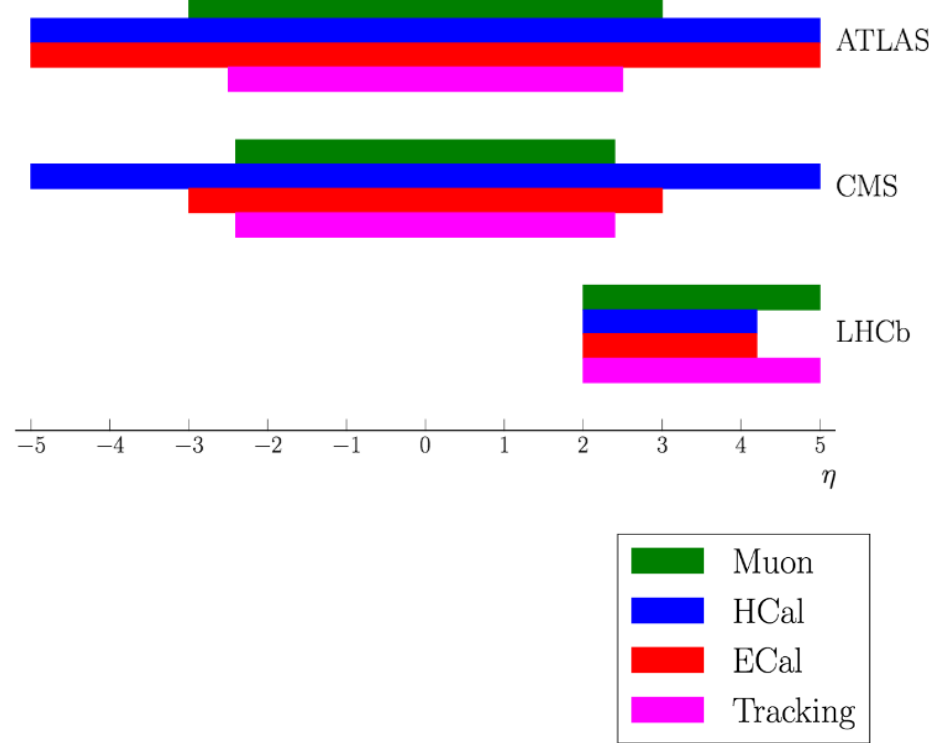
# Heavy-flavour production



Fabio Ferrari on behalf of the LHCb collaboration  
Università di Bologna and INFN – Sezione di Bologna  
Beauty 2018

# Introduction

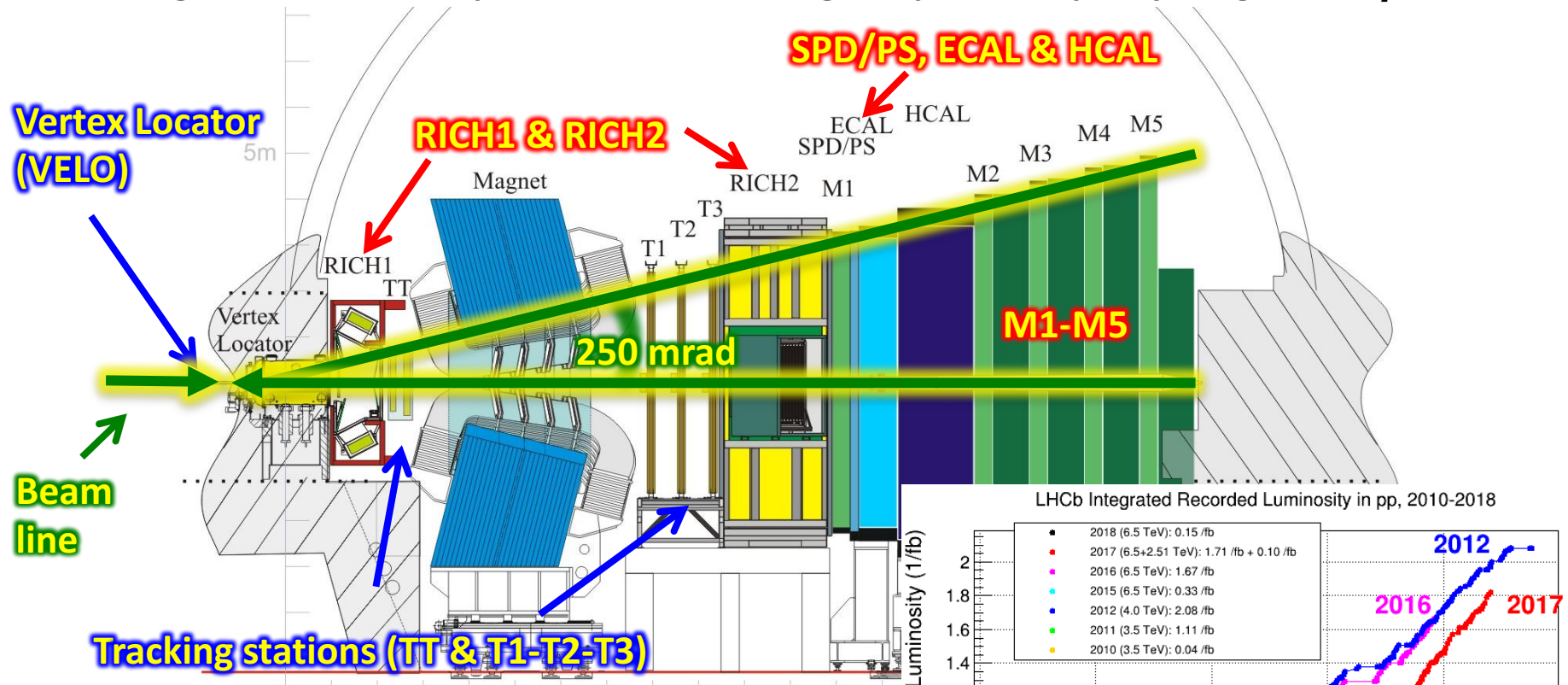
- LHCb geometrical acceptance allows to perform **unique measurements** in the **forward region**
  - Complementary to ATLAS/CMS
- Today results
  - $\gamma$  production in  $pp$  collisions at  $\sqrt{s} = 13$  TeV
  - $B^+$  production cross-section in  $pp$  collision at  $\sqrt{s} = 7$  TeV and  $\sqrt{s} = 13$  TeV
  - $D_s^+$  production asymmetry at  $\sqrt{s} = 7$  TeV and  $\sqrt{s} = 8$  TeV



# The LHCb detector

J. Instrum. 3 (2008) S08005

Single-arm forward spectrometer covering the pseudorapidity range  $2 < \eta < 5$



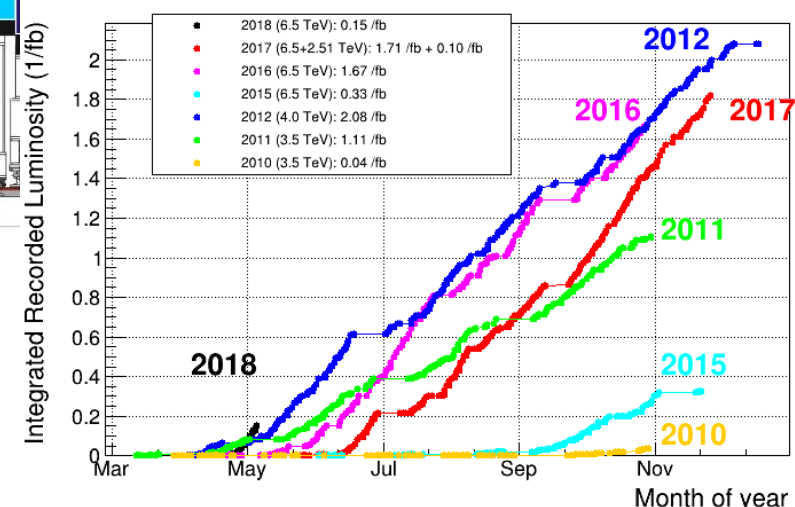
LHCb integrated luminosity 5m

$1 \text{ fb}^{-1}$  @  $\sqrt{s} = 7 \text{ TeV}$

$2 \text{ fb}^{-1}$  @  $\sqrt{s} = 8 \text{ TeV}$

$2 \text{ fb}^{-1}$  @  $\sqrt{s} = 13 \text{ TeV}$  (2015-2016)

Magnet polarity can be switched when needed



A scenic view of a coastal resort. In the foreground, there's a sandy beach with numerous orange and white striped umbrellas. To the right, there are several swimming pools, some with water slides, surrounded by lounge chairs and palm trees. In the background, there are green hills covered in dense vegetation, and a few buildings are visible at the base of the hills. The sky is clear and blue.

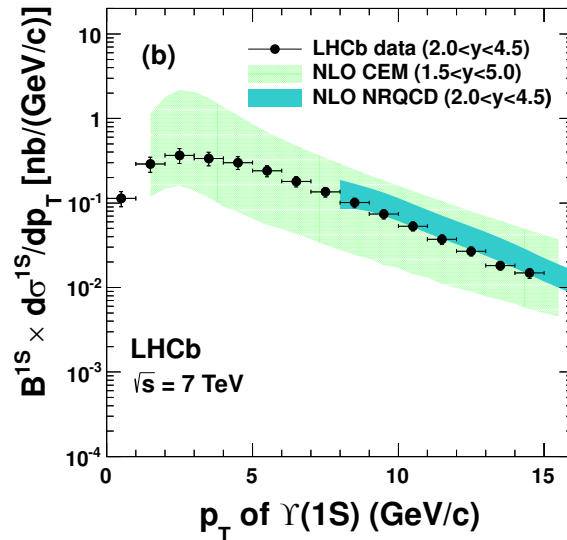
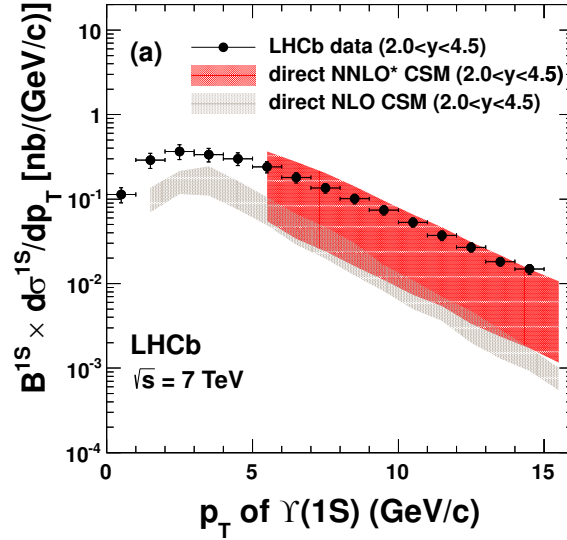
$\Upsilon$  production in  $pp$  collisions at  
 $\sqrt{s} = 13 \text{ TeV}$

# Motivations

LHCb-PAPER-2018-002

- Study of heavy quarkonium production in high-energy collisions provides information on QCD
- Several models proposed to describe underlying dynamics
  - Colour singlet model (CSM)
  - Non-relativistic QCD (NRQCD)
  - Colour Evaporation Model (CEM)
- Calculate ratio with respect to 7 and 8 TeV results → cancel majority of systematic uncertainties

Eur. Phys. J. C72 (2012) 2025



# Analysis strategy

LHCb-PAPER-2018-002

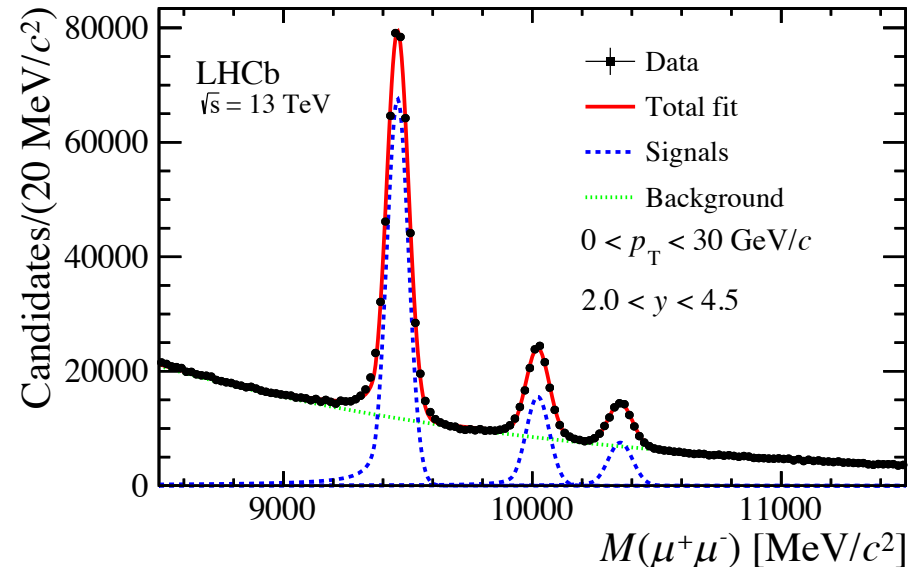
- Measure differential production cross-section as function of  $p_T$  and  $y$  multiplied by the  $\Upsilon(nS) \rightarrow \mu^+ \mu^-$  branching fractions
- Data sample
  - $277 \text{ pb}^{-1}$  @  $\sqrt{s} = 13 \text{ TeV}$
- Calculate

$$\frac{d^2\sigma}{dydp_T} \times B(\Upsilon \rightarrow \mu^+ \mu^-) = L \times \varepsilon_{tot}(p_T, y) \times \Delta y \times \Delta p_T$$

Total integrated luminosity

Total efficiency

- Detector acceptance, selection and trigger efficiencies from simulation
- Tracking efficiency from simulation and corrected with data-driven method
- Particle identification efficiency from calibration samples



Signal yields  
 $398 \cdot 10^3 \Upsilon(1S)$   
 $100 \cdot 10^3 \Upsilon(2S)$   
 $51 \cdot 10^3 \Upsilon(3S)$

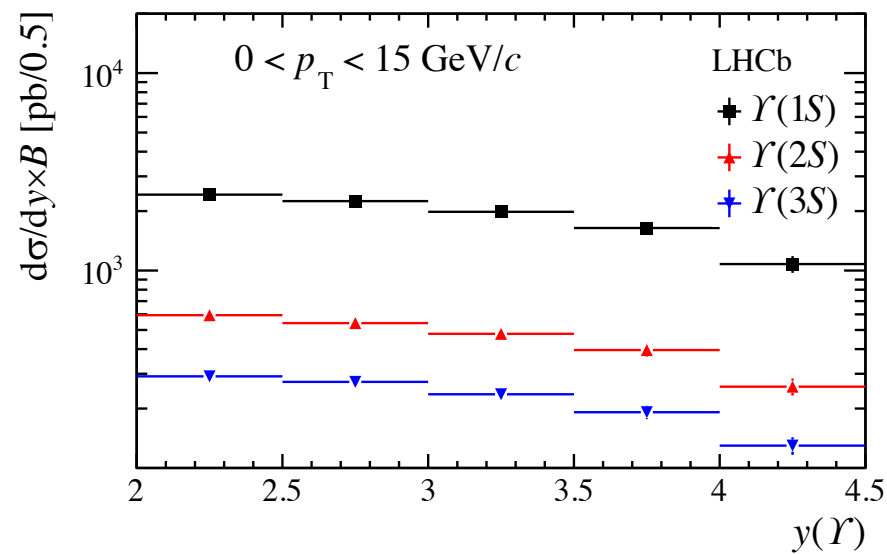
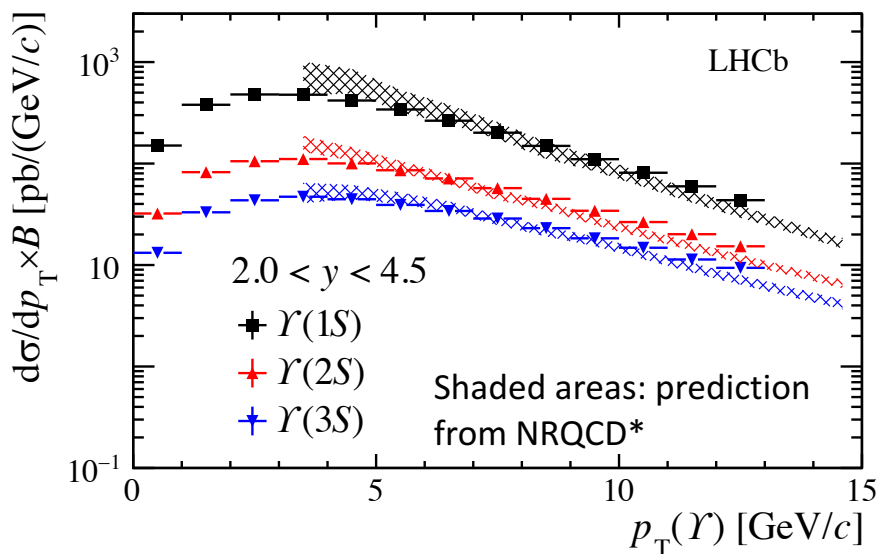
Bin width

## Integrated results

$$\mathcal{B}(\Upsilon(1S) \rightarrow \mu^+ \mu^-) \times \sigma(\Upsilon(1S), 0 < p_T < 15 \text{ GeV}/c, 2 < y < 4.5) = 4687 \pm 10 \pm 294 \text{ pb}$$

$$\mathcal{B}(\Upsilon(2S) \rightarrow \mu^+ \mu^-) \times \sigma(\Upsilon(2S), 0 < p_T < 15 \text{ GeV}/c, 2 < y < 4.5) = 1134 \pm 6 \pm 71 \text{ pb}$$

$$\mathcal{B}(\Upsilon(3S) \rightarrow \mu^+ \mu^-) \times \sigma(\Upsilon(3S), 0 < p_T < 15 \text{ GeV}/c, 2 < y < 4.5) = 561 \pm 4 \pm 36 \text{ pb}$$

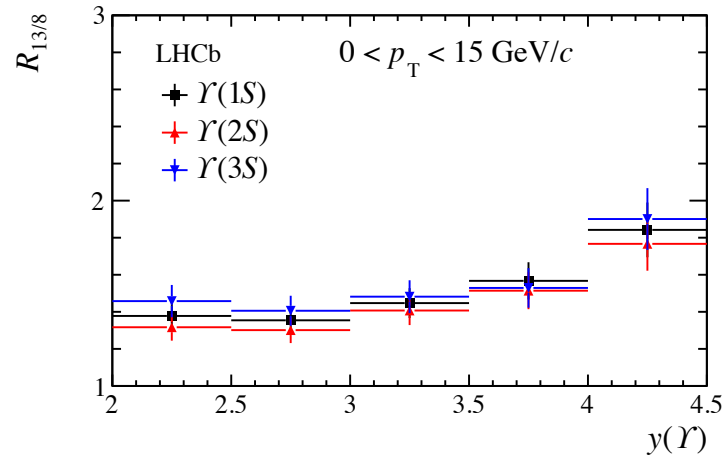
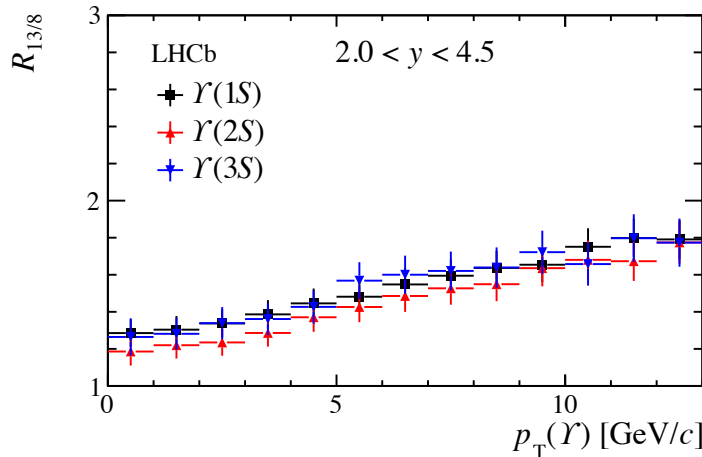


- Measurements are dominated by systematic uncertainty
  - Main contribution due to trigger efficiency and luminosity determination
- Prediction from NRQCD provides a reasonable description of data at high  $p_T$

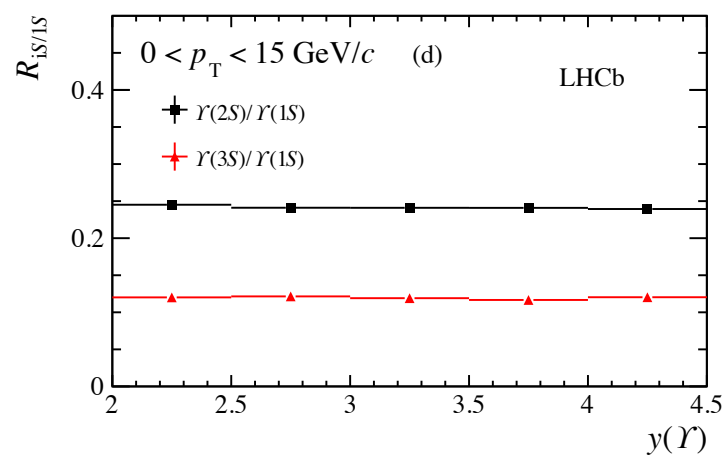
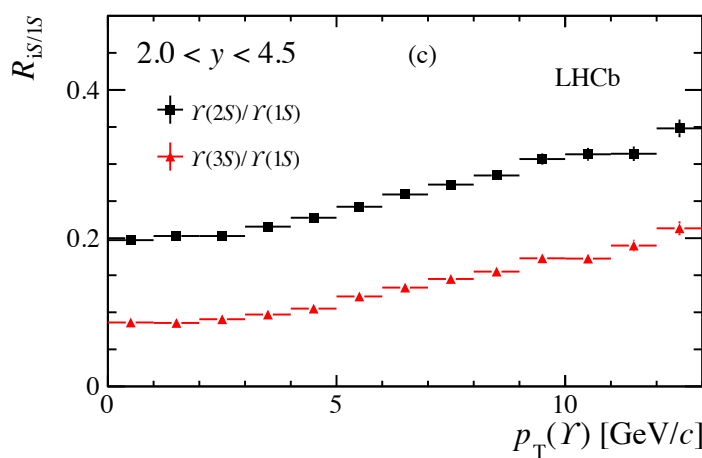
# Ratios

LHCb-PAPER-2018-002

- 13/8 TeV ratio increasing as a function of  $p_T$  and  $y$



- iS to 1S ratio increasing as function of  $p_T$  and flat as function of  $y$



A scenic view of a coastal town with hills in the background and a beach in the foreground.

**$B^+$  production cross-section in  
pp collision at  $\sqrt{s} = 7$  TeV and  
 $\sqrt{s} = 13$  TeV**

# Motivations

JHEP 12 (2017) 026

- Precise measurement of production cross-section of  $B^+$  mesons provides important test for QCD calculations
- Complementary phase-space with respect to ATLAS and CMS allow to test theory at low  $p_T$ /high  $y$
- Possibility to measure ratios at different centre-of-mass energies to largely cancel theory and experimental uncertainties

## Current experimental status

	Luminosity	$\sqrt{s}$ (TeV)	Range	Cross Section ( $\mu\text{b}$ )
CDF [2]	$739 \text{ pb}^{-1}$	1.96	$p_T > 6 \text{ GeV}/c,$ $ y  < 1$	$2.78 \pm 0.24$
CMS [3]	$5.8 \text{ pb}^{-1}$	7	$p_T > 5 \text{ GeV}/c,$ $ y  < 2.4$	$28.1 \pm 2.4 \pm 2.0 \pm 3.1$
ATLAS [4]	$2.4 \text{ fb}^{-1}$	7	$9 < p_T < 120 \text{ GeV}/c,$ $ y  < 2.25$	$10.6 \pm 0.3 \pm 0.7 \pm 0.2 \pm 0.4$
LHCb [5]	$35 \text{ pb}^{-1}$	7	$0 < p_T < 40 \text{ GeV}/c,$ $2 < y < 4.5$	$41.5 \pm 1.5 \pm 3.1$
LHCb [6]	$362 \text{ pb}^{-1}$	7	$0 < p_T < 40 \text{ GeV}/c,$ $2 < y < 4.5$	$38.9 \pm 0.3 \pm 2.8$

<sup>2</sup> Phys. Rev. D75 (2007) 012010

<sup>3</sup> Phys. Rev. Lett. 106 (2011) 112001

<sup>4</sup> JHEP 10 (2013) 042

<sup>5</sup> JHEP 04 (2012) 93

<sup>6</sup> JHEP 08 (2013) 117

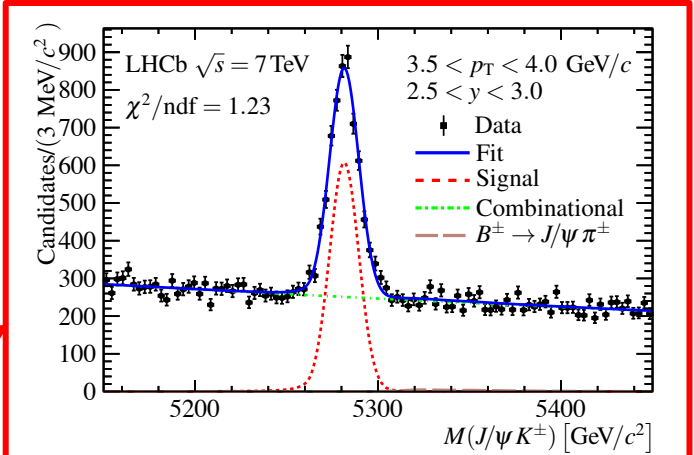
# Analysis

JHEP 12 (2017) 026

## • Data sample

- $1 \text{ fb}^{-1}$  @  $\sqrt{s} = 7 \text{ TeV}$
- $0.3 \text{ fb}^{-1}$  @  $\sqrt{s} = 13 \text{ TeV}$

Signal yields in each bin obtained by means of extended unbinned maximum likelihood fits to  $m(J/\psi K^\pm)$  distribution



## • Master formula

$$\frac{d^2\sigma}{dydp_T} = \mathcal{L} \times \varepsilon_{tot} \times \mathcal{B}(B^\pm \rightarrow J/\psi K^\pm) \times \mathcal{B}(J/\psi \rightarrow \mu^+ \mu^-) \times \Delta y \times \Delta p_T$$

Total integrated luminosity

Obtained combining Belle\* and BaBar\*\* measurements

Taken from PDG

Bin width

### Total efficiency

- Detector acceptance, selection and trigger efficiencies from simulation
- Tracking efficiency from simulation and corrected with data-driven method
- Particle identification efficiency from calibration samples

\*Phys. Rev. D67 (2003) 032003

\*\*Phys. Rev. Lett. 94 (2005) 141801

# Results

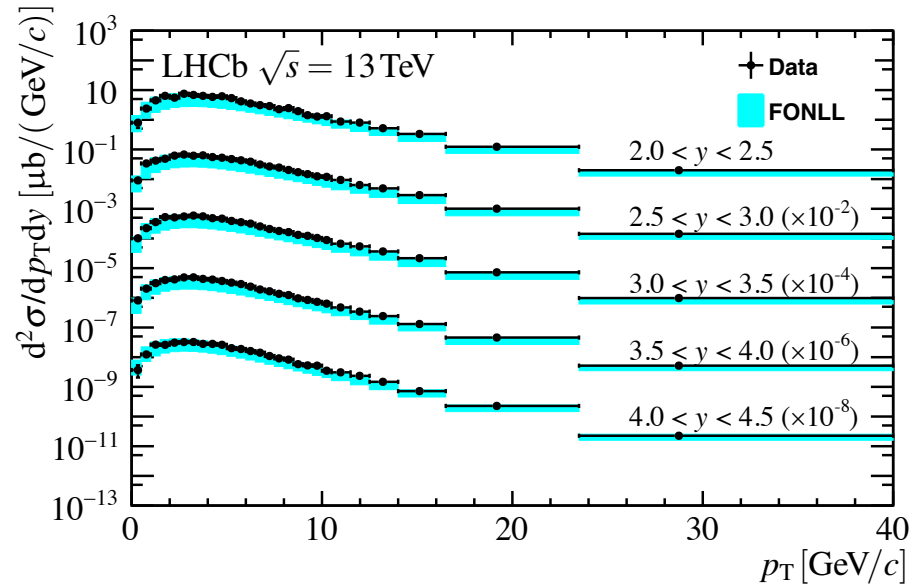
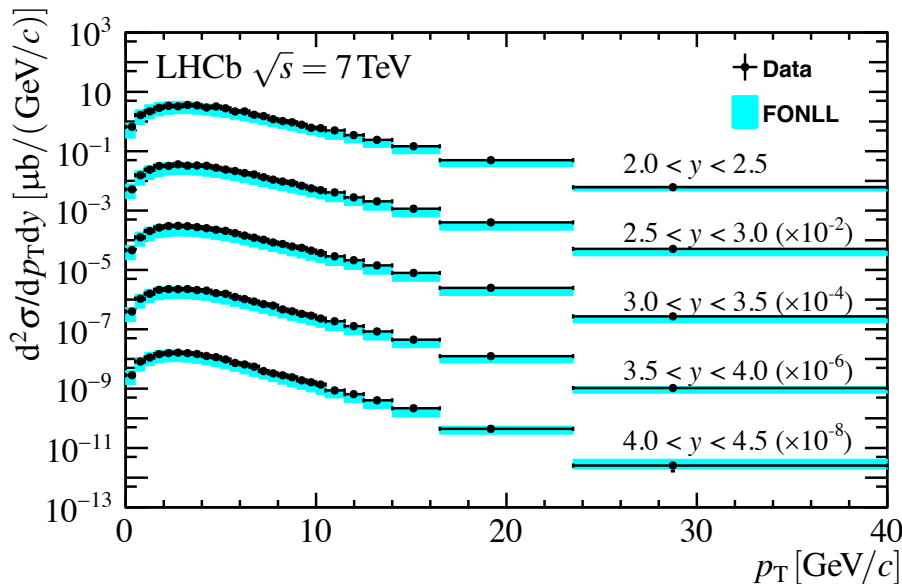
JHEP 12 (2017) 026

## Integrated results

$$\sigma(pp \rightarrow B^\pm X, \sqrt{s} = 7 \text{ TeV}) = 43.0 \pm 0.2 \pm 2.5 \pm 1.7 \mu\text{b}$$

$$\sigma(pp \rightarrow B^\pm X, \sqrt{s} = 13 \text{ TeV}) = 86.6 \pm 0.5 \pm 5.4 \pm 3.4 \mu\text{b}$$

- The results are in good agreement with FONLL predictions

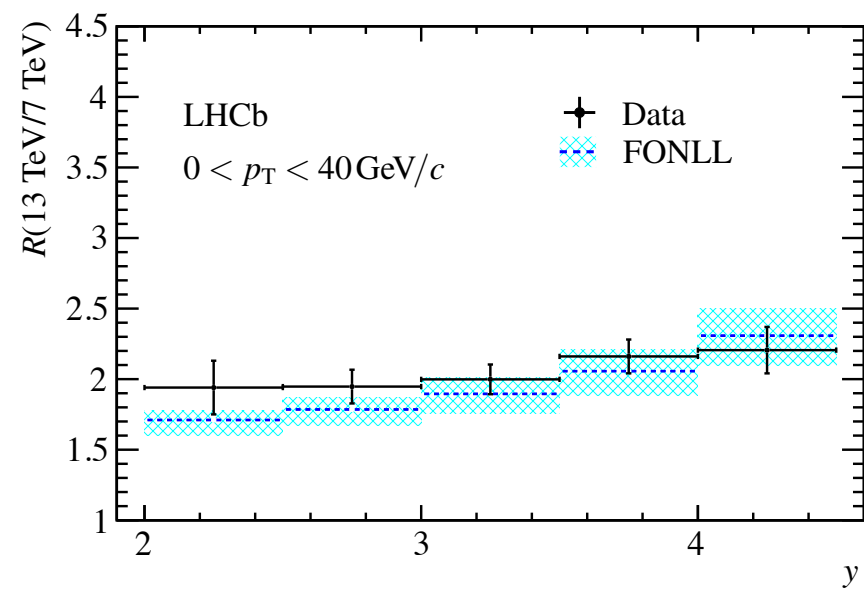
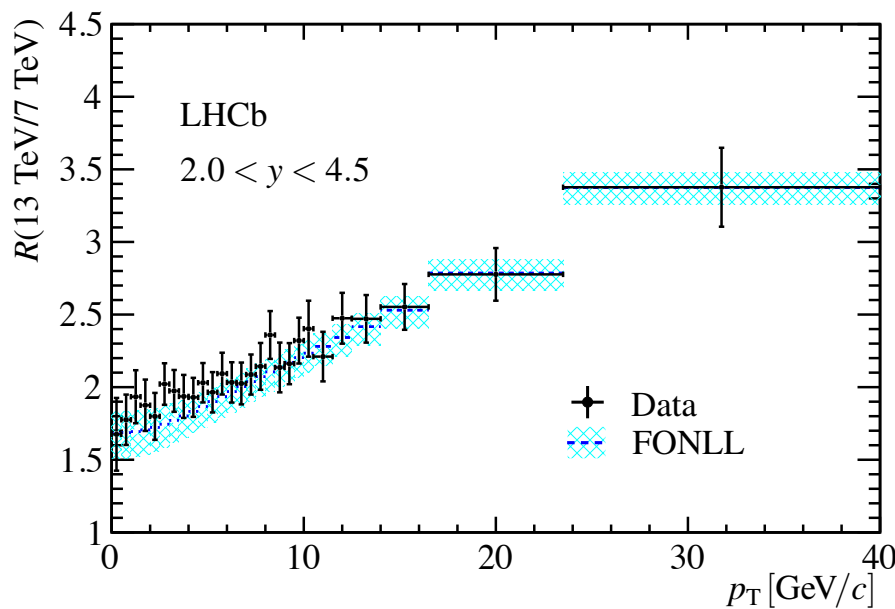


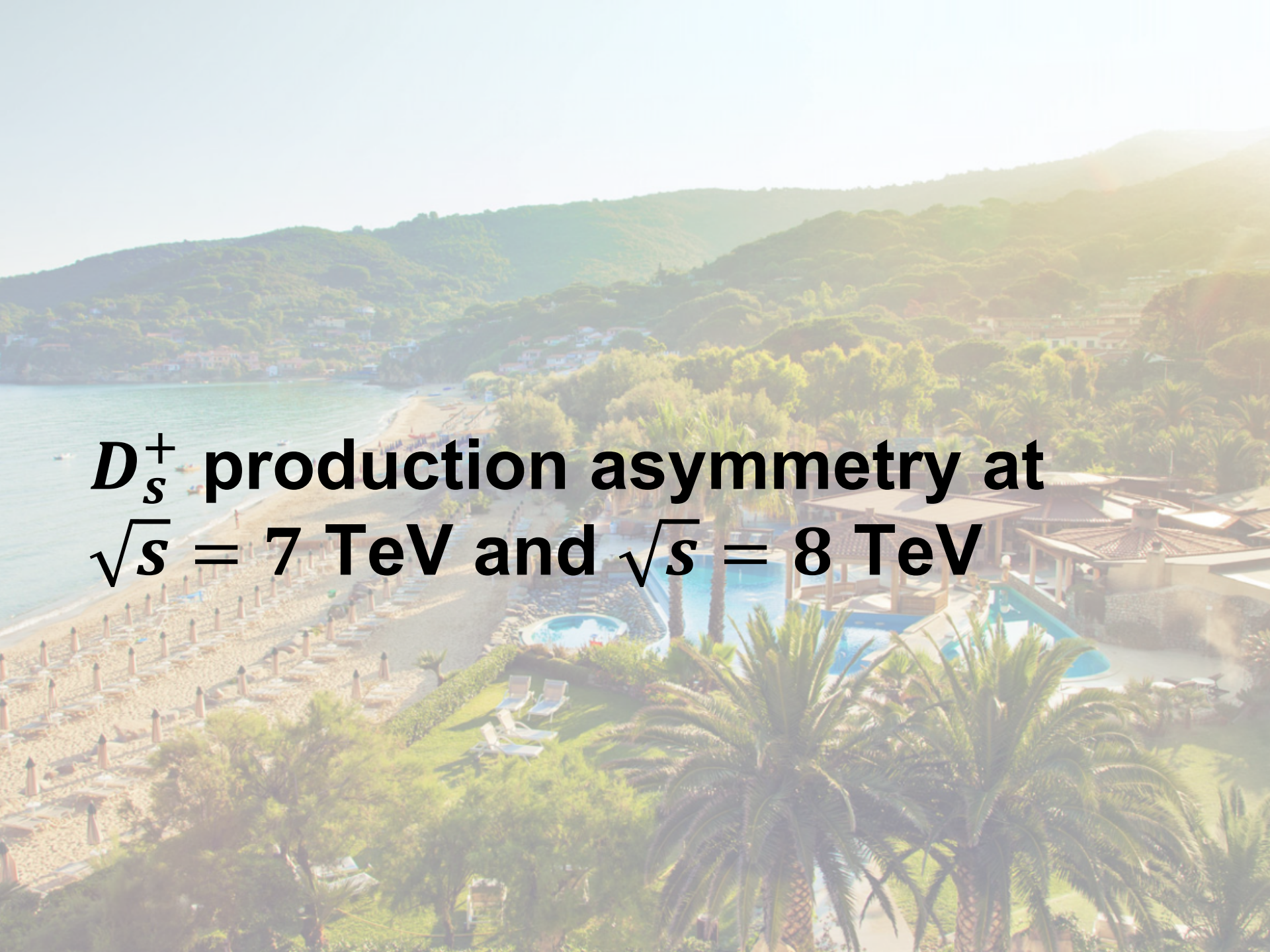
FONLL predictions: Eur. Phys. J C75 (2015) 610

# 13/7 TeV ratio

JHEP 12 (2017) 026

- Also the ratio at the two different centre-of-mass energies (13 and 7 TeV) is compatible with FONLL predictions
  - FONLL predictions from Eur. Phys. J C75 (2015) 610



A scenic view of a coastal town with hills in the background and a beach in the foreground.

**$D_s^+$  production asymmetry at  
 $\sqrt{s} = 7 \text{ TeV}$  and  $\sqrt{s} = 8 \text{ TeV}$**

# Motivation

LHCb-PAPER-2018-010

- $b$  and  $c$ -hadrons are **not expected** to be produced at the **same rate** with respect to  $\bar{b}$  and  $\bar{c}$ -hadrons in  **$p\bar{p}$  collisions**
  - $u$  and  $d$  quarks from the **remnants** of the colliding protons can combine with  $\bar{b}$  and  $\bar{c}$  quarks to form a **meson**, whereas the opposite **can't happen**
  - This has to be **compensated** by an opposite asymmetry in the other **species**



- Production asymmetry measurements are a **key ingredient** to perform **CP violation** measurements
  - One needs to disentangle the physical CP asymmetry from **other spurious effects**
- Production asymmetries are defined as:

$$A_P(D_{(s)}^+) = \frac{\sigma(D_{(s)}^+) - \sigma(D_{(s)}^-)}{\sigma(D_{(s)}^+) + \sigma(D_{(s)}^-)}$$

where  $\sigma$  is the inclusive prompt production cross-section

# Analysis

\*Phys. Rev. D95 (2017) 052005

Phys. Lett. B774 (2017) 139

Phys. Rev. Lett. 114 (2015) 041601

LHCb-PAPER-2018-010

- Data sample:  $D_s^+ \rightarrow \phi(\rightarrow K^+K^-)\pi^+$ 
  - $1 \text{ fb}^{-1}$  @  $\sqrt{s} = 7 \text{ TeV}$
  - $2 \text{ fb}^{-1}$  @  $\sqrt{s} = 8 \text{ TeV}$
- Production asymmetry can be expressed as the sum of various components

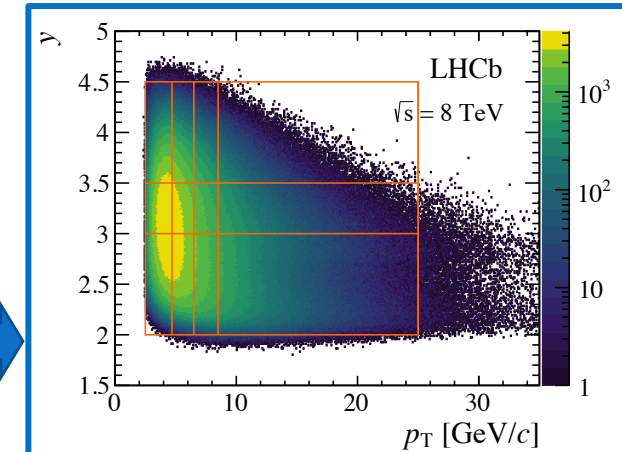
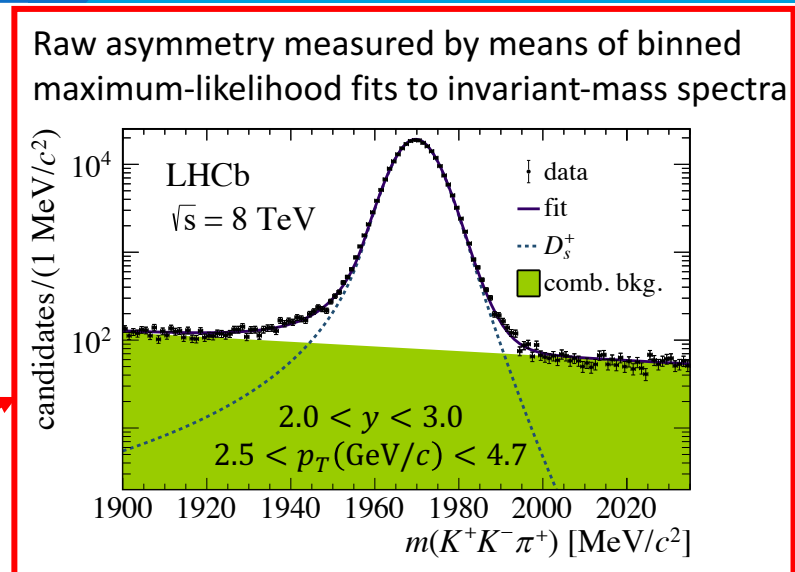
$$A_P(D_s^+) = \frac{1}{1 - f_{bkg}} (A_{raw} - A_D - f_{bkg} A_P(B))$$

Fraction of secondary  $D_s^+$  decays

Sum of various detection asymmetries

b-hadron production asymmetry\*

Measurement performed as a function of  $p_T$  and  $y$



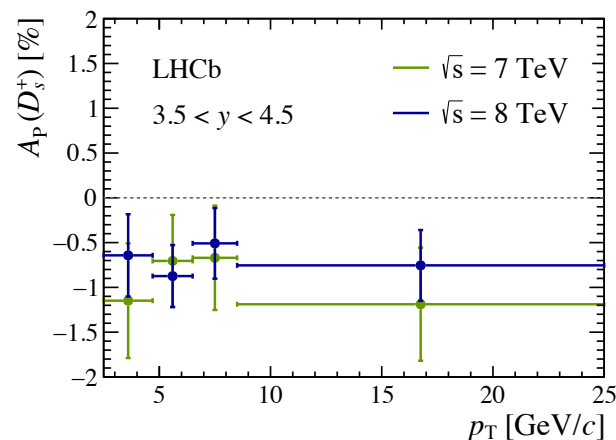
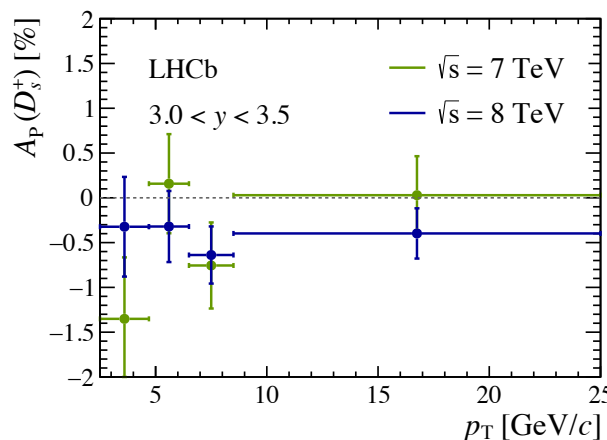
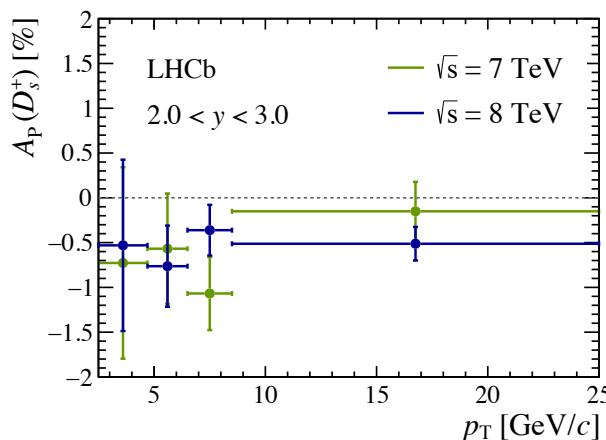
# Results

LHCb-PAPER-2018-010

- Integrating in the range  $2.5 < p_T(\text{GeV}/c) < 25$  and  $2.0 < y < 4.5$  the  $D_s^+$  production asymmetry is found to be

$$A_P(D_s^+) = (-0.52 \pm 0.13 \text{ (stat)} \pm 0.10 \text{ (syst)})\%$$

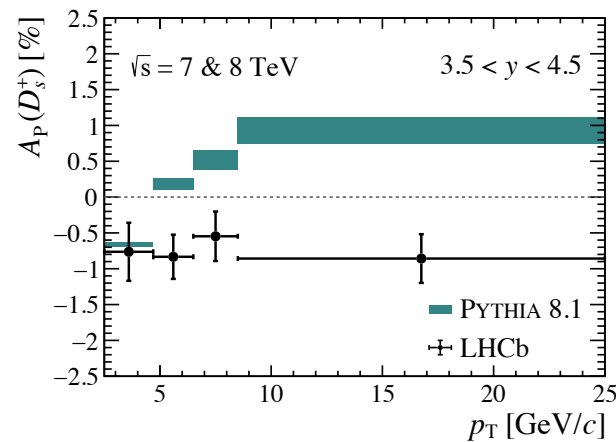
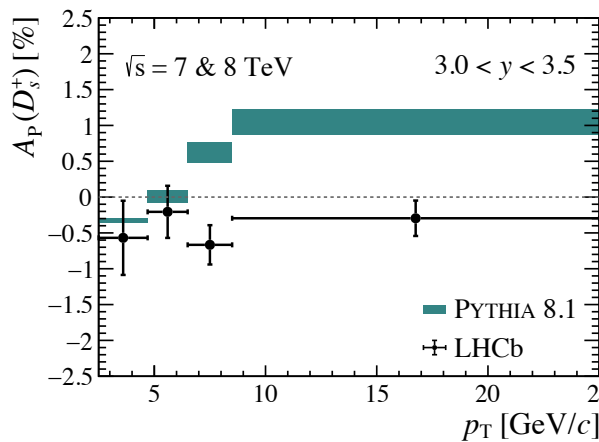
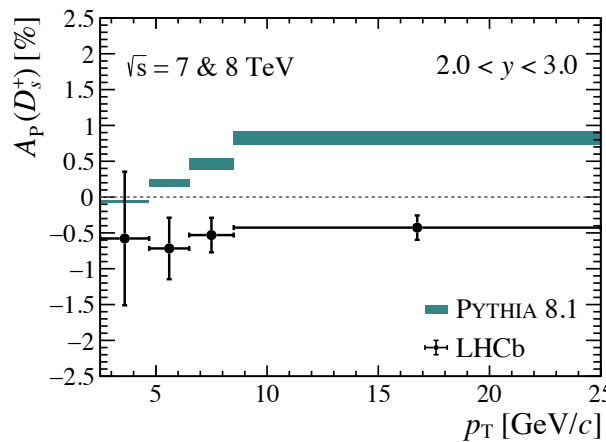
- Evidence for nonzero asymmetry at  $3.3\sigma$  level
- No dependence on kinematics observed



# Comparison with Pythia 8.1

LHCb-PAPER-2018-010

- The Pythia event generator includes models accounting for mechanisms that cause production asymmetries
- Pythia simulation shows a strong dependence on both  $p_T$  and  $y$ , that is not observed in data



- Results obtained in this analysis can be used to tune production models for various event generators

# Conclusions

- Several results presented today, exploiting both Run 1 and Run 2 data samples collected by LHCb
- LHCb is testing theoretical model predictions in a unique kinematic region
  - Interplay with theory community very important
- Many more measurements are coming, using Run 2 and 5 TeV data sets
- Run 2 samples allow to perform analyses in final states that were limited by statistics in Run 1
- Several new results are coming this summer... stay tuned...!

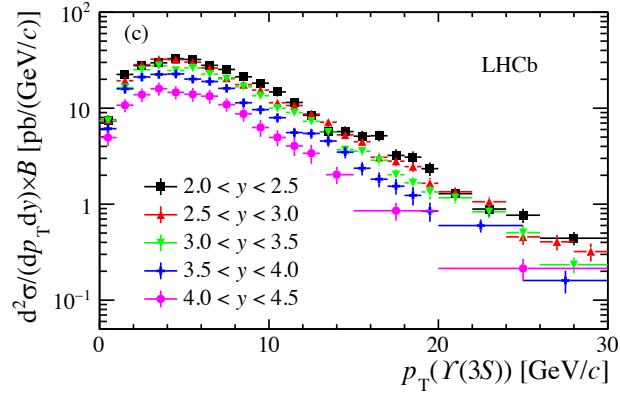
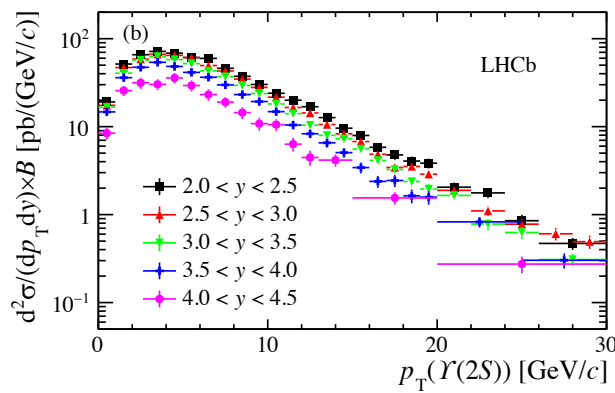
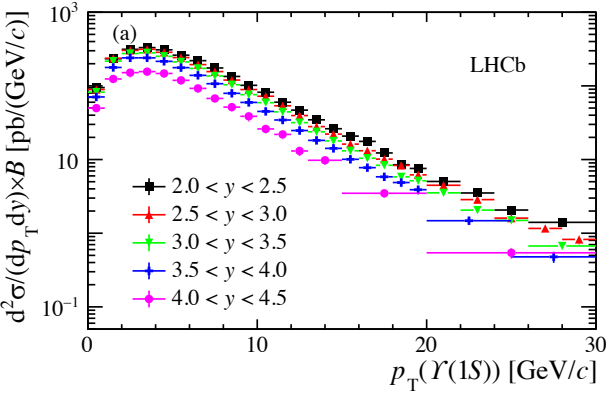
The background image shows a beautiful coastal scene. In the foreground, there's a sandy beach with numerous orange and white striped umbrellas. To the right of the beach, there's a large swimming pool complex with several pools and a wooden pavilion. The middle ground features a lush green hillside covered in dense vegetation and a few small buildings. The background consists of more hills and a clear blue sky.

**Thanks for your attention!**

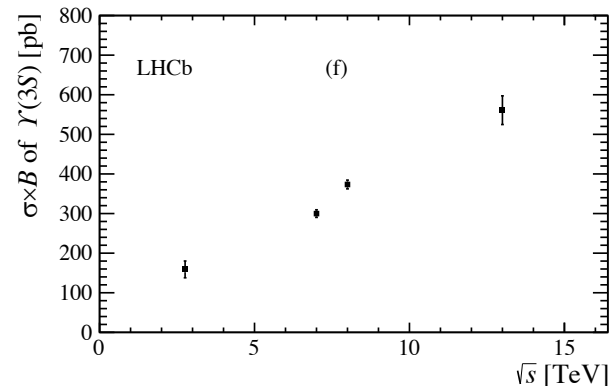
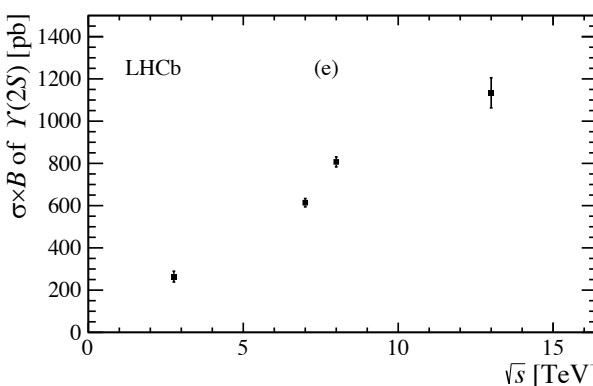
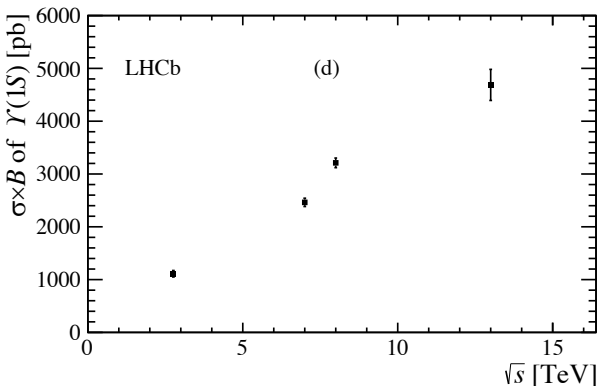
# **Backup**

# $\Upsilon(nS)$ production

- Double-differential cross-sections multiplied by dimuon branching fractions as a function of  $p_T$



- Production cross-sections multiplied by dimuon branching fractions integrated over  $0 < p_T(\text{GeV}/c) < 15$  and  $2.0 < y < 4.5$



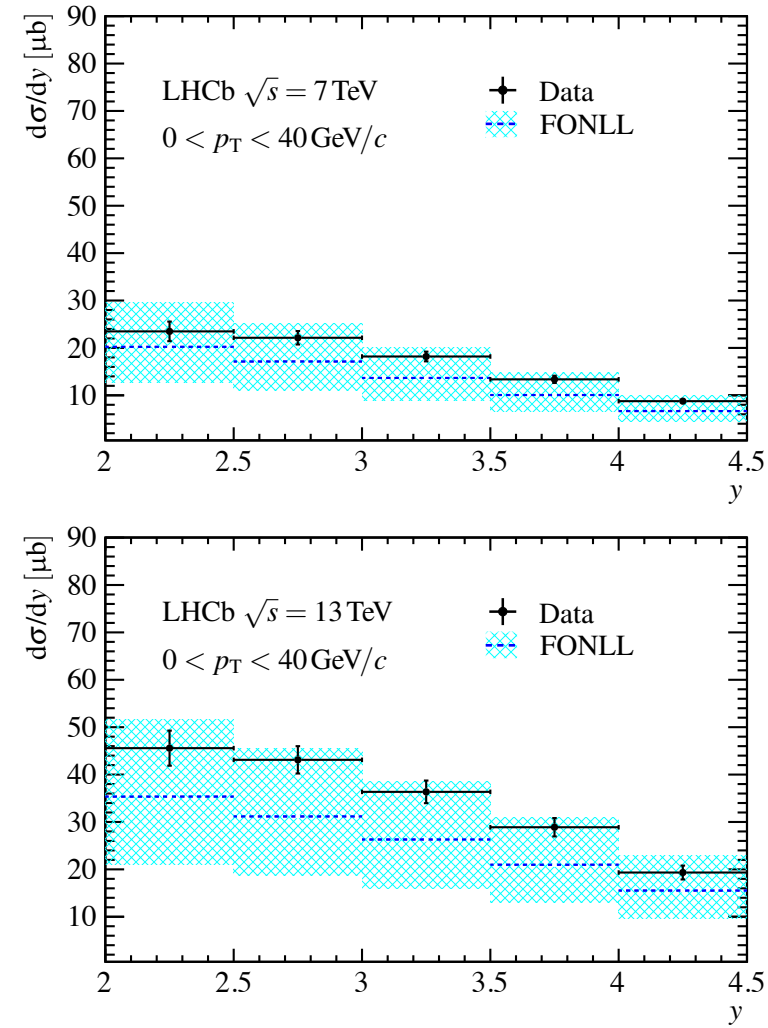
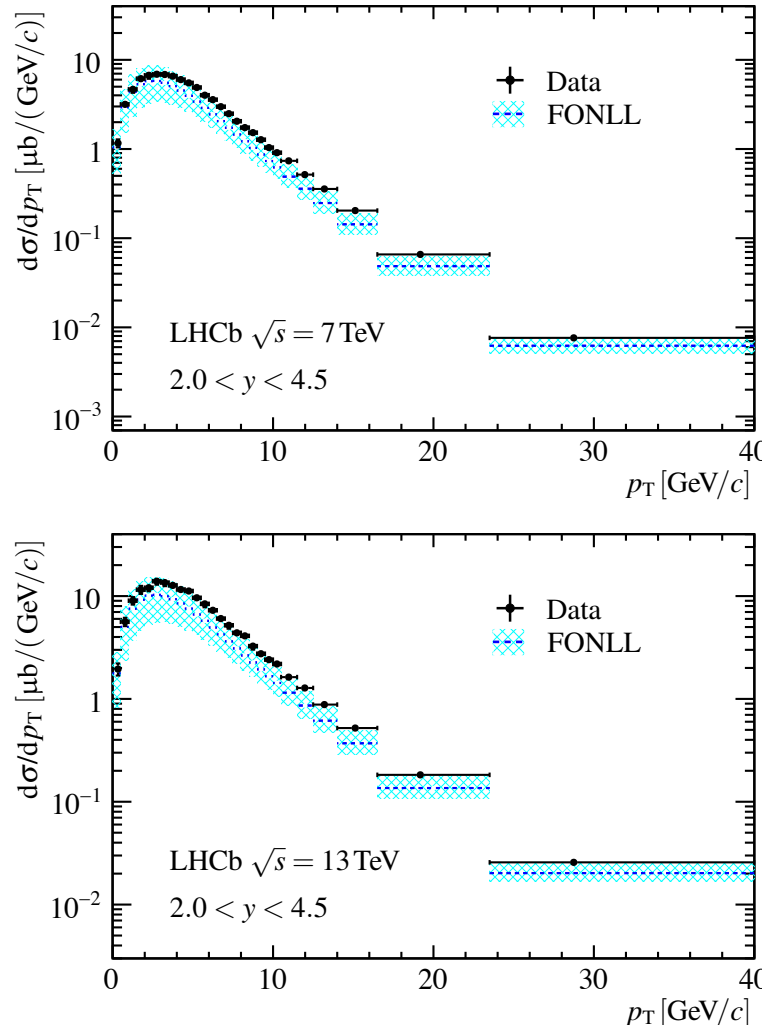
# $\Upsilon(nS)$ production

- Summary of systematic uncertainties

Source	$\Upsilon(1S)$	$\Upsilon(2S)$	$\Upsilon(3S)$	Comment
Fit models	1.9	1.8	2.5	Correlated
Simulation statistics	$0.4 - 4.6$	$0.5 - 5.1$	$0.5 - 4.4$	Bin dependent
Global event requirements	0.6	0.6	0.6	Correlated
Trigger	$3.9 - 9.8$ $(0.1 - 6.6)$	$3.9 - 9.8$ $(0.2 - 6.4)$	$3.9 - 9.8$ $(0.2 - 6.5)$	Bin dependent
Tracking	$\oplus 2 \times 0.8$	$\oplus 2 \times 0.8$	$\oplus 2 \times 0.8$	Correlated
Muon identification	$0.1 - 7.9$	$0.1 - 7.6$	$0.2 - 8.5$	Correlated
Vertexing	0.2	0.2	0.2	Correlated
Kinematic spectrum	$0.0 - 1.1$	$0.0 - 2.2$	$0.0 - 2.5$	Bin dependent
Radiative tail	1.0	1.0	1.0	Correlated
Luminosity	3.9	3.9	3.9	Correlated
Total	$6.2 - 14.3$	$6.2 - 14.6$	$6.4 - 14.9$	Correlated

# $B^+$ production cross-section

- Measured differential cross-section as a function of  $p_T$  and  $y$



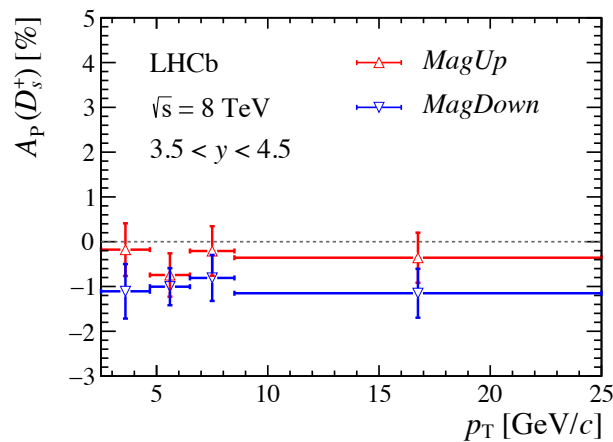
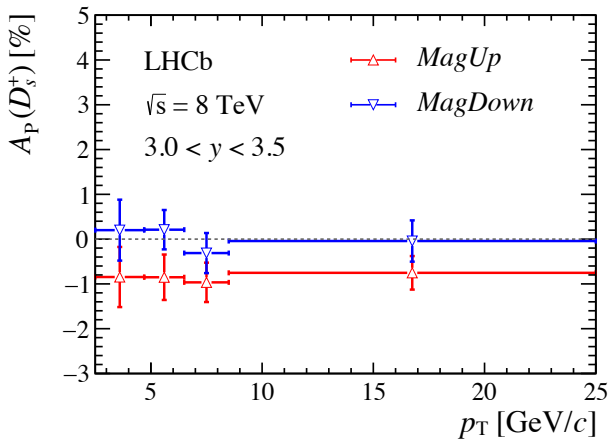
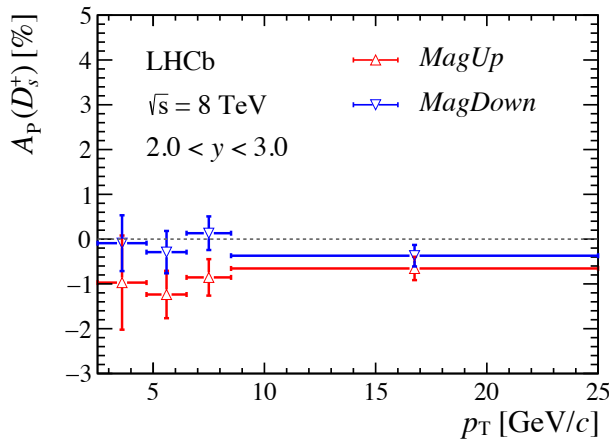
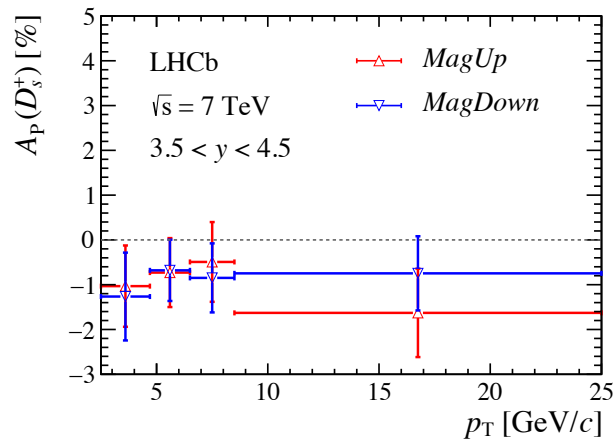
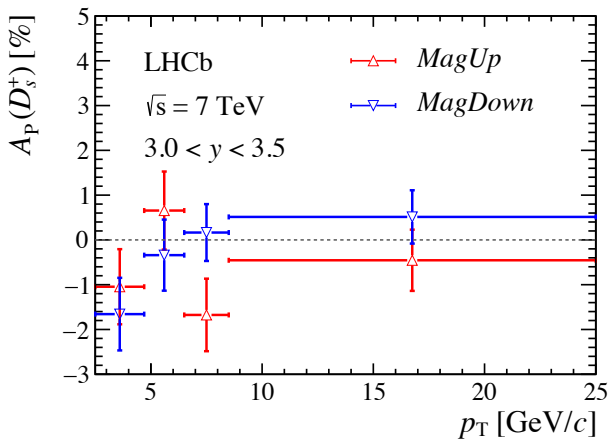
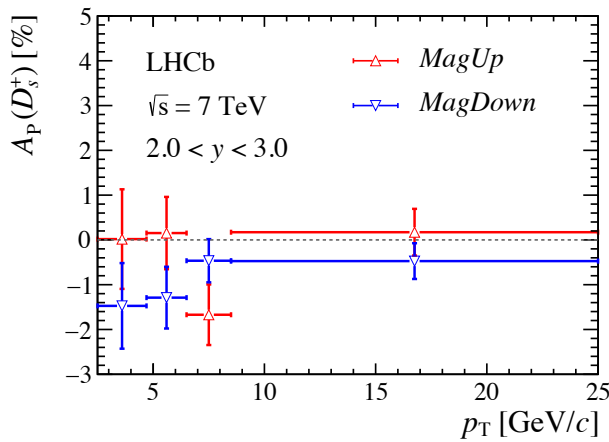
# $B^+$ production cross-section

- Summary of systematic uncertainties

Sources	Uncertainty (%)		
	7 TeV	13 TeV	$R(13 \text{ TeV}/7 \text{ TeV})$
Luminosity	1.7	3.9	3.4
Branching fractions	3.9	3.9	0.0
Binning	2.6	2.7	0.0
Mass fits	2.7	1.3	1.5
Acceptance	0.2	0.1	0.2
Reconstruction	0.1	0.1	0.2
Track	1.6	2.6	1.0
PID	0.4	0.1	0.4
Trigger	3.5	2.6	4.4
GEC	0.7	0.7	1.0
Selection	1.0	1.1	0.1
Weighting	0.2	0.2	0.3
Total	7.0	7.4	5.9

# $D_s^+$ production asymmetry

- Production asymmetry as a function of  $p_T$  in bins of  $y$ , separated by magnet polarity



# $D_s^+$ production asymmetry

- Numerical results

7 TeV

$p_T$ [ GeV/c ]	$y$		
	2.0 – 3.0	3.0 – 3.5	3.5 – 4.5
2.5 – 4.7	$-0.73 \pm 0.62 \pm 0.87$	$-1.35 \pm 0.55 \pm 0.41$	$-1.15 \pm 0.60 \pm 0.23$
4.7 – 6.5	$-0.57 \pm 0.51 \pm 0.35$	$0.16 \pm 0.49 \pm 0.25$	$-0.70 \pm 0.48 \pm 0.17$
6.5 – 8.5	$-1.07 \pm 0.40 \pm 0.08$	$-0.76 \pm 0.47 \pm 0.09$	$-0.67 \pm 0.56 \pm 0.16$
8.5 – 25.0	$-0.15 \pm 0.32 \pm 0.08$	$0.03 \pm 0.42 \pm 0.11$	$-1.19 \pm 0.63 \pm 0.09$

8 TeV

$p_T$ [ GeV/c ]	$y$		
	2.0 – 3.0	3.0 – 3.5	3.5 – 4.5
2.5 – 4.7	$-0.53 \pm 0.40 \pm 0.87$	$-0.32 \pm 0.37 \pm 0.41$	$-0.64 \pm 0.40 \pm 0.23$
4.7 – 6.5	$-0.76 \pm 0.29 \pm 0.35$	$-0.32 \pm 0.30 \pm 0.25$	$-0.87 \pm 0.30 \pm 0.17$
6.5 – 8.5	$-0.36 \pm 0.27 \pm 0.08$	$-0.64 \pm 0.31 \pm 0.09$	$-0.51 \pm 0.36 \pm 0.16$
8.5 – 25.0	$-0.51 \pm 0.17 \pm 0.08$	$-0.40 \pm 0.26 \pm 0.11$	$-0.75 \pm 0.39 \pm 0.09$

7+8 TeV

$p_T$ [ GeV/c ]	$y$		
	2.0 – 3.0	3.0 – 3.5	3.5 – 4.5
2.5 – 4.7	$-0.58 \pm 0.34 \pm 0.87$	$-0.57 \pm 0.31 \pm 0.41$	$-0.76 \pm 0.34 \pm 0.23$
4.7 – 6.5	$-0.72 \pm 0.25 \pm 0.35$	$-0.21 \pm 0.26 \pm 0.25$	$-0.83 \pm 0.26 \pm 0.17$
6.5 – 8.5	$-0.53 \pm 0.23 \pm 0.08$	$-0.67 \pm 0.26 \pm 0.09$	$-0.55 \pm 0.30 \pm 0.16$
8.5 – 25.0	$-0.43 \pm 0.15 \pm 0.08$	$-0.30 \pm 0.22 \pm 0.11$	$-0.86 \pm 0.33 \pm 0.09$